Available online at www.sciencedirect.com
ScienceDirect
Surface & Coatings Technology 202 (2008) 4572–4577
SURFACE & COATINGS TECHNOLOGY
www.elsevier.com/locate/surfcoat

Fatigue and corrosion fatigue behavior of an AA6063-T6 aluminum alloy coated with a WC–10Co–4Cr alloy deposited by HVOF thermal spraying

C.J. Villalobos-Gutiérrez [a], G.E. Gedler-Chacón [a], J.G. La Barbera-Sosa [b], A. Piñeiro [b], M.H. Staia [b], J. Lesage [c], D. Chicot [c], G. Mesmacque [c], E.S. Puchi-Cabrera [b,d,*]

[a] School of Mechanical Engineering, Faculty of Engineering, Universidad Central de Venezuela, Caracas, Venezuela
[b] School of Metallurgical Engineering and Materials Science, Faculty of Engineering, Universidad Central de Venezuela, Caracas, Venezuela
[c] Laboratoire de Mécanique de Lille, Université de Lille 1, Mécanique des Materiaux, UMR CNRS 8107, Villeneuve D'Ascq, 59650, France
[d] Venezuelan National Academy for Engineering and Habitat, Palacio de las Academias, Caracas, 1010, Postal Address 1723, Venezuela

Available online 10 April 2008

Abstract

The present investigation has been conducted in order to study the fatigue and corrosion fatigue behavior of an AA6063-T6 aluminum alloy substrate coated with a WC–10Co–4Cr deposited by HVOF thermal spraying. It has been determined that the deposition of such a coating on the aluminum substrate gives rise to significant gains in fatigue life in comparison with the uncoated substrate, when testing is carried out both in air and in a 3 wt.% NaCl solution. It has been shown that during testing in air, the fatigue gain ranges between ~540 and 4300%, depending on the maximum alternating stress applied to the material. Larger fatigue gains are associated with low alternating stresses. Also, when fatigue testing is conducted in the NaCl solution, the gain in fatigue resistance varies between ~620 and 1460%. Fatigue cracks have been observed to initiate at the coating surface and then grow towards the substrate after propagating through the entire coating thickness. Crack growth along the coating has been observed to occur mainly along the regions formed by the agglomeration of W and W–Co–Cr-rich particles, flanking the tougher Co–Cr-rich areas. Although in the present work residual stresses were not measured, it is believed that the gain in fatigue life of the coating–substrate system is due to the presence of compressive residual stresses within the coating which hinder fatigue crack propagation. The deposition of the coating does not give rise to significant changes in the static mechanical properties and hardness of the aluminum alloy substrate. It has been observed that the WC–10Co–4Cr coating displays a significant indentation size effect and has a mean hardness of ~9.4 GPa.

Keywords: AA6063-T6 aluminum alloy; WC–10Co–4Cr coating; HVOF thermal spray; Fatigue; Corrosion fatigue; Hardness

1. Introduction

6XXX aluminum alloys are very important engineering materials employed in a variety of applications which include automotive, construction, chemical, petrochemical, cryogenics, transportation equipment, etc. These materials exhibit relatively high strength to weight ratio, good corrosion resistance and high thermal conductivity, among other attractive properties. However, due to their low hardness and wear and abrasion resistance, the application of these materials to sliding parts is quite limited. Traditionally, the improvement of the surface properties of the aluminum alloys, and particularly of those involved in aircraft and aerospace applications, has been the use of electrolytic hard chromium deposition (EHC). However, the strong environmental regulations issued in the past few years to decrease significantly the emissions of the highly toxic hexavalent chromium, synthesized during the deposition of EHC, have led to the development of different technologies also able to improve the surface properties of such materials, but more friendly from the environmental point of view [1–8].

In general, the mechanical and surface properties of parts and components depend on the specific applications for which these have been designed. Thus, while wear and corrosion properties are improved through surface treatments such as EHC, electroless Ni–P (EN) and thermal spraying, components

* Corresponding author. School of Metallurgical Engineering and Materials Science, Faculty of Engineering, Universidad Central de Venezuela, Caracas, Venezuela. Tel.: +58 212 7539017.
E-mail address: epuchi@reacciun.ve (E.S. Puchi-Cabrera).

0257-8972/$ - see front matter © 2008 Elsevier B.V. All rights reserved.
doi:10.1016/j.surfcoat.2008.04.044

subjected to cyclic loading are expected to have high strength and fatigue resistance. Thus, the study of the fatigue and corrosion fatigue behavior of coated materials is of utmost importance, since an increase in surface properties could be achieved at the expense of a decrease in fatigue strength. In the past few years, a number of research studies have been conducted in order to investigate the fatigue performance of aluminum alloys coated by means of EN, thermal spraying and PVD deposition [9–17].

One of the first reports on the effects of different spraying parameters of high velocity oxygen fuel deposition (HVOF) on the fatigue resistance of coated aluminum samples is that of Brandt [9]. A thorough investigation of this subject was subsequently reported by McGrann et al. [10] who studied the effect of the HVOF deposition of a WC–17Co coating onto a 6061-T6511 aluminum substrate, with particular emphasis on the analysis of the effect of the through-thickness residual stresses. In this investigation the fatigue tests were conducted in bending and the residual stresses measured by the modified layer removal method. These authors showed that the fatigue resistance of the uncoated substrate is higher than that of the HVOF coated alloy and concluded that the increase in the compressive residual stress in the coating increased the number of cycles to failure of the substrate specimens.

More recently, Connoly et al. [11] have reported the results of an investigation aimed at determining the effect of aluminum coatings deposited by flame arc, atmospheric plasma and HVOF on the three-point bend fatigue behavior of un-corroded and pre-corroded AA2024-T3 substrate samples. The comparison made by these authors of the microstructures, mechanical properties and fatigue properties of the coated samples revealed that HVOF is the most promising thermal spray process for the deposition of aluminum coatings, and, in particular, HVOF coatings greatly increase the fatigue and pre-corroded fatigue lifetimes of the AA2024-T3 substrate.

Camargo et al. [15] also conducted an investigation in order to evaluate a WC–Co coating applied by HVOF, used for the replacement of anodizing. To carry out the appropriate comparison, the study involved the growth of anodic films on a 7050-T7451 aluminum alloy substrate by sulfuric acid anodizing, chromic acid anodizing and hard anodizing. According to these authors, anodic films give rise to a decrease in the axial fatigue strength of the substrate. Also, the experimental results revealed an increase in the fatigue strength of the substrate associated with the WC–17Co coating, although a reduction in fatigue life occurred in the shot peened and coated condition.

Puchi-Cabrera et al. [16] have recently conducted an investigation aimed at studying the effect of a WC–12Co alloy deposited by plasma spraying on the fatigue and corrosion fatigue properties of a 7075-T6 aluminum alloy, as part of its validation as a viable replacement of electrolytic hard chromium plating for aircraft applications. These authors reported that coating this substrate alloy with a deposit of ~50 μm gives rise to a significant decrease in the fatigue and corrosion fatigue properties of the substrate coating system in comparison with the uncoated substrate. Particularly, when the coated substrate was tested in air at maximum alternating stress in the range 219–377 MPa, the fatigue life debit was found to vary between 86 and 73% in comparison with the uncoated substrate. Also, it was determined that if the substrate coating system was tested in a 3% NaCl solution in the same range of alternating stress, the fatigue life debit varied between 23 and 73%. However, at alternating stresses less than 200 MPa the coated system behaved as the uncoated substrate.

Thus, the present investigation has been carried out in order to analyze the fatigue and corrosion fatigue behavior of an AA6063-T6 aluminum alloy coated with a WC–10%Co–4%Cr coating of approximately 250 μm in thickness, deposited by HVOF thermal spraying, and compare it with that of the uncoated substrate tested under the same conditions. Tensile and fatigue testing has been complemented with extensive SEM analysis of the fractured surfaces in order to obtained some information regarding the damage mechanisms associated with crack nucleation and growth in the coating–substrate system. No attempt has been made in order to study separately the corrosion behavior of the coated substrate in the absence of cyclic loading, which has been widely investigated by other authors [4,18–21].

2. Experimental techniques

This study was carried out with samples of an AA6063-T6 aluminum alloy (Al–0.40Si–0.68Mg–0.35Fe–0.1Cu–0.1Mn–0.1Cr–0.1Ti–0.1Zn (wt.%), as indicated by the supplier), which were machined from bars of ~12.7 mm diameter. Tensile and fatigue ("hourglass") specimens were machined according to the ASTM B 557 and E 206-72 standards, respectively [22,23]. The specimens were machined carefully in order to avoid the introduction of residual stresses. To accomplish this objective, during the turning operation the depth of cut of the material was reduced continuously employing a turret lath at low speed. The samples were subsequently ground with successive SiC papers grit 600–1200 (average diameter of 14.5–6.5 μm, respectively) and final polishing with alumina of 0.3 mm. This procedure allowed the achievement of a 'mirror-like' finish in the fatigue specimens and ensured the removal of the remaining circumferential notches that could act as stress concentrators during the fatigue tests.

Each Wöhler curve presented in this work required testing not less than 20 fatigue samples, whereas the static mechanical properties determined in tension, not less than 3 samples. Additionally, cylindrical specimens were machined in order to the conduct composition analysis of the coating and micro-indentation tests. The HVOF deposition of the WC–10Co–4Cr, commercially known as AlloyH654 (Praxair), was carried out at an industrial facility (Plasmatec Ingenieros, C. A., Guarenas, Edo. Miranda, Venezuela). The deposition parameters are given in Table 1.

In the as-sprayed condition, the specimens presented an average roughness of $R_a \cong 5.5$ μm, which was reduced by polishing to $R_a \cong 2$ μm, previous to fatigue testing. Tensile tests were conducted on a 8502 Instron machine (Canton, MA, USA) at a cross head speed of 3 mm/s. Fatigue in air and in a 3 wt.%

Table 1
Main parameters involved in HVOF deposition process

Coating	WC–Co–Cr
Thermal spray gun	TAFA HVOF JP-5000
Spraying distance (mm)	380±10
Powder feeding rate (g min^{-1})	83
Particle size range (μm)	20–70
Kerosene flux (l min^{-1})	0.32
Oxygen flux (l min^{-1})	897
N_2 (carrier gas) flux (l min^{-1})	~11
Combustion pressure inside the chamber (MPa)	0.65
Fuel/Oxygen ratio	0.73

NaCl solution were carried out under rotating–bending conditions, on a RBF-200 Fatigue Dynamics (Walled Lake, MI, USA) equipment at maximum alternating stresses of 118, 144, 168 and 177 MPa and a frequency of 50 Hz. Five samples were tested at each alternating stress. After fatigue testing, selected fracture surfaces were analyzed by means of SEM techniques. Observations were conducted on the fracture plane of the specimens. The hardness of the coating was evaluated by means of Vickers indentation employing loads of 25, 50, 100, and 200 g. At least, ten measurements were conducted at each load.

3. Results and discussion

3.1. Coating characterization

The mean thickness of the deposited coating was of ~250 μm. Fig. 1 illustrates a representative cross section of a coated sample where a lamellar structure with lamellas parallel to the substrate surface and unmelted particles typical of this type of coatings are clearly observed. The coating–substrate interface is observed to be quite irregular, possibly due to the impact of the high velocity particles that constitute the coating, on the relatively soft aluminum substrate. Since the samples had a "mirror-like" finish before deposition, it is evident that the substrate had undergone a severe plastic deformation during the coating process. However, such deformation enhances the mechanical bonding and adhesion of the coating to the substrate. The EDS analysis of the deposit indicated that it is mainly composed of WC (88%), as well as other phases rich in Co (6%), Cr (4%) and Ni (2%), the latter considered in the present case as an impurity element.

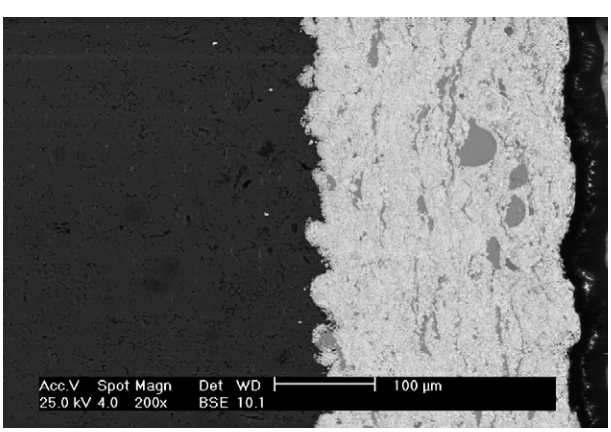

Fig. 1. Representative cross section of a coated sample showing the microstructure and thickness (~250 μm) of the AlloyH654 deposit.

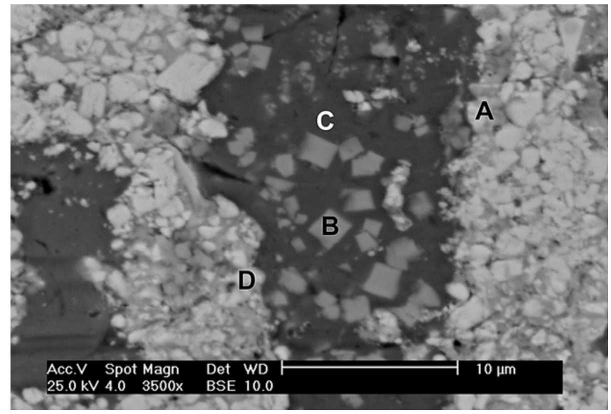

Fig. 2. Detailed view of the coating microstructure. Four different regions with distinct composition have been identified.

Fig. 2 illustrates a detailed view of the coating, where it can be clearly observed that the different components of the coating are distributed quite heterogeneously. Four different regions, identified as A, B, C and D, have been identified on the micrograph. Regions A and D are observed to be formed by an agglomeration of white-grey particles of variable sizes between ~1 and 5 μm. Some of them (Region D) presented a very high content of W, whereas in region A the particles were observed to be composed mainly of W, Co and Cr. The region identified as C has a dark color and was observed to be rich in Cr, with less Co and W. Within this zone and identified as region B, squared particles of ~2–3 μm in size mainly composed of Ni, Cr, W and Fe, can be clearly seen. According to Sobolev et al. [24], the main phases that are present in this kind coating are WC, W_2C and Cr_7C_3. In general, it has been observed that the particles present in the coating tend to be larger near the surface and smaller as the coating–substrate interface is approach.

The evaluation of the substrate hardness in cross section after deposition indicated that this property did not change significantly in comparison with the uncoated substrate,

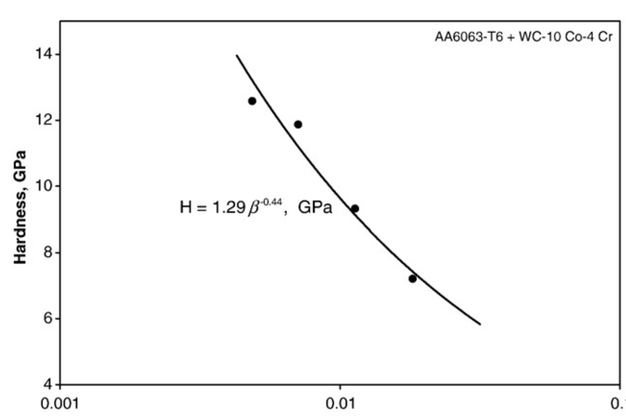

Fig. 3. Change in hardness with R.I.D. (β) for the WC–10Co–4Cr coating.

which points out that the deposition process, besides the plastic deformation of the substrate surface layers, does not give rise to profound changes in its microstructure and T6 condition. Fig. 3, on the other hand, illustrates the change in hardness with the relative indentation depth

Fig. 3 illustrates the change in hardness with the Relative Indentation Depth (R.I.D.), β, for the WC–10Co–4Cr coating. As can be seen from the figure, the coating experiences a significant decrease in hardness as β increases. However, since all the hardness values have been determined in the range of $\beta<0.1$, the substrate influence in the hardness value is negligible. Therefore, the change in hardness with β represents and indentation size effect (ISE) that can be described by means of Meyer's law [25] as:

$$H = H_0 \beta^{n-2} \quad (1)$$

From the experimental data it has been determined that $H_0 = 1.29$ GPa and $n = 1.56$. It can be seen from the above figure that the mean hardness of the coating, derived from the experimental data, is in the range of ~9.4 GPa. La Barbera-Sosa et al. [26] have also reported the occurrence of a significant ISE in other HVOF thermally sprayed coatings such as Colmonoy 88 and AlloyH275, which have been explained in terms of the heterogeneity of the local microstructure involved in the indentation volume of the coating and the occurrence of microcracking during loading.

3.2. Tensile and fatigue tests

Tensile tests conducted on the AA6063-T6 aluminum alloy samples indicated that this material has a yield stress of ~190 MPa and an ultimate tensile stress of ~228 MPa. On the other hand, the tests carried out on the coated specimens indicated that such properties apparently decreased to ~166 and ~194 MPa, respectively. Also, the hardness tests conducted on the aluminum alloy substrate before and after deposition allowed the determination of values of 0.75 and 0.73 GPa, respectively, indicating that such a property remains almost unchanged after deposition of the coating. The fact that the hardness of the substrate before and after deposition is almost the same suggests that the decrease in tensile properties after deposition is simply an artifact of the way in which such stresses are computed for the coated substrate, which is carried out by including the coating thickness in the calculation of the cross sectional area of the specimen. The inclusion of the coating thickness in the computation of such an area assumes that the coating acts as a load-carrying element of the composite material, which is not the case. Given the limited ductility of the coating, it would be expected that at strains above those associated with the elastic limit, the HVOF deposit fractured and delaminated from the substrate, leaving the uncoated substrate as the only load-carrying element of the coating–substrate system.

Fig. 4 illustrates the change in the number of cycles to fracture (N_f), as a function of the maximum alternating stress applied to the material (S), presented in the form of a typical Wöhler plot and includes the data corresponding to the tests conducted in air and in a 3 wt.% NaCl solution for both the uncoated and coated substrate. The S versus N_f data have been described by means of a simple parametric relationship of the form:

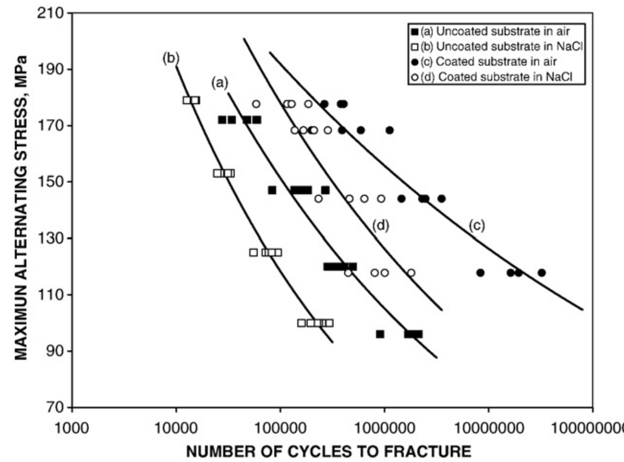

Fig. 4. Wöhler curves corresponding to the uncoated and coated substrate tested in air and NaCl solution.

$$S = A N_f^{-m}, \quad \text{MPa} \quad (2)$$

In the above equation, A represents the fatigue resistance and m the fatigue exponent. The above figure clearly shows that coating the aluminum substrate with this WC–10Co–4Cr alloy deposited by HVOF, gives rise to a significant increase in its fatigue and corrosion fatigue resistance, as compared with the uncoated substrate, in agreement with the results of Camargo et al. [15]. When fatigue tests are carried out in air, the increase in fatigue resistance is much more significant at low maximum alternating stresses, of ~4300%. At elevated maximum alternating stresses, the fatigue gain is of 540%. Also, when tests are conducted in the NaCl solution at low maximum alternating stresses, the gain in fatigue resistance is of ~1460%, whereas at elevated alternating stress it is of ~620%.

This behavior could be attributed to the presence of compressive residual stresses in the coating which arise during its deposition. As reported by McGrann et al. [9], WC–17Co coatings deposited by HVOF onto aluminum samples were observed to be under different compressive residual stresses, depending on the deposition parameters, whose average magnitude varied from ~80 to 760 MPa. As can be clearly observed in Fig. 4, the standard deviation of the number of cycles to fracture increases moderately as the maximum alternating stress applied to the material decreases.

3.3. Fractographic analysis

Selected samples tested in fatigue both in air and in the NaCl solution were analyzed after fracture by SEM, both on the main fracture plane and in cross section. Fig. 5a and b illustrates the fracture surface of a fatigue coated sample tested

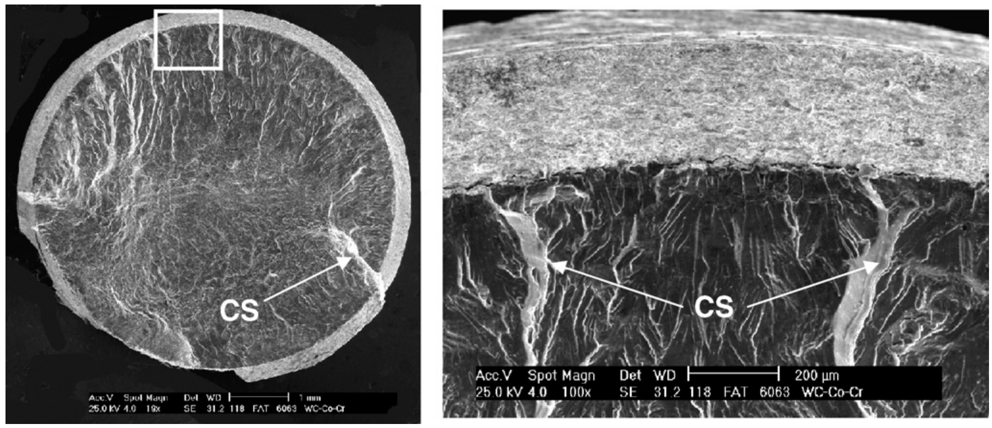

Fig. 5. (a) Fracture surface of fatigue coated sample tested at 118 MPa, which failed at ~19.5×10^6 cycles. The presence of a number of cleavage steps and extensive delamination of the coating are clearly visible. (b) Detailed view of the area indicated in (a), showing a crack nucleation site. Cleavage steps (CS) are also identified.

in air at a maximum alternating stress of 118 MPa. Fig. 5a shows a general view of the fracture surface on which a number of cleavage steps (CS) can be observed, indicating that the fracture of the specimen occurred by the nucleation and propagation of a number of cracks. Such a behavior was also observed in the samples tested at other different maximum alternating stresses and it was found that the number of fatigue cracks nucleated at the specimens periphery increase as the maximum alternating stress also increases. Fig. 5b illustrates a detailed view of the area depicted in (a), where the cleavage steps can be seen more clearly. This region was identified as a fatigue crack nucleation site and the coating is observed to have remained adhered to the substrate.

Fig. 6, on the other hand, illustrates a cross section view of a sample tested in air at 118 MPa, which failed at 19.5×10^6 cycles. This figure clearly shows that fatigue cracks are nucleated at the surface of the coating and subsequently propagate towards the substrate. Particularly, in the present case, the crack has hardly reached the coating–substrate interface and crack propagation has taken place mainly through the regions formed by the agglomeration of white-grey W and W–Co–Cr-rich particles, identified as A and D in Fig. 3. The crack is also observed to

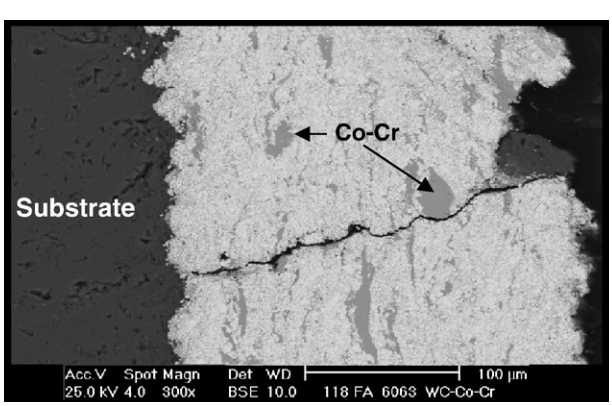

Fig. 6. Cross section view of a sample tested in air at an alternating stress of 118 MPa, which failed at ~19.5×10^6 cycles. Crack propagation is observed to occur from the coating surface towards the aluminum substrate.

flank the presumably tougher Co–Cr regions identified as B and C on the same micrograph.

Fig. 7a illustrates the fracture surface of a coated sample tested in the NaCl solution at a maximum alternating stress of 178 MPa, which failed at 128,100 cycles. Here, it is clearly observed that the ductile fracture zone (DFZ) is located at the center of the fracture surface, which indicates that a large number of fatigue cracks were nucleated at the periphery of the sample and propagated towards its center. Also, extensive delamination of the coating can be seen. Fig. 7b shows a detailed view of the area depicted in (a), at one of the crack nucleation sites. Here, the coating is observed to have delaminated from the substrate and propagation of the fatigue cracks along the latter gives rise to a highly faceted surface near the interface, which indicates an intergranular crack growth mode.

4. Conclusions

Coating the AA6063-T6 aluminum alloy with the WC–10Co–4Cr deposit studied in this investigation leads to significant gains in fatigue life in comparison with the uncoated substrate, when testing is carried out both in air and in a 3 wt.% NaCl solution. During testing in air, the fatigue gain has been found to range between ~540 and 4300%, depending on the maximum alternating stress applied to the material. Larger fatigue gains are associated with low alternating stresses. Also, when fatigue testing is conducted in the NaCl solution, the gain in fatigue resistance varies between ~620 and 1460%. Fatigue cracks were observed to nucleate at the coating surface and then propagate towards the substrate after consuming the entire coating thickness. Crack growth along the coating was observed to occur mainly along the regions formed by the agglomeration of white-grey W and W–Co–Cr-rich particles, flanking the tougher Co–Cr-rich areas. Although in the present work residual stresses were not measured, it is believed that the gain in fatigue life of the coating–substrate system is due to the presence of compressive residual stresses within the coating which hinder fatigue crack propagation. The deposition of the coating does not give rise to significant changes in the static

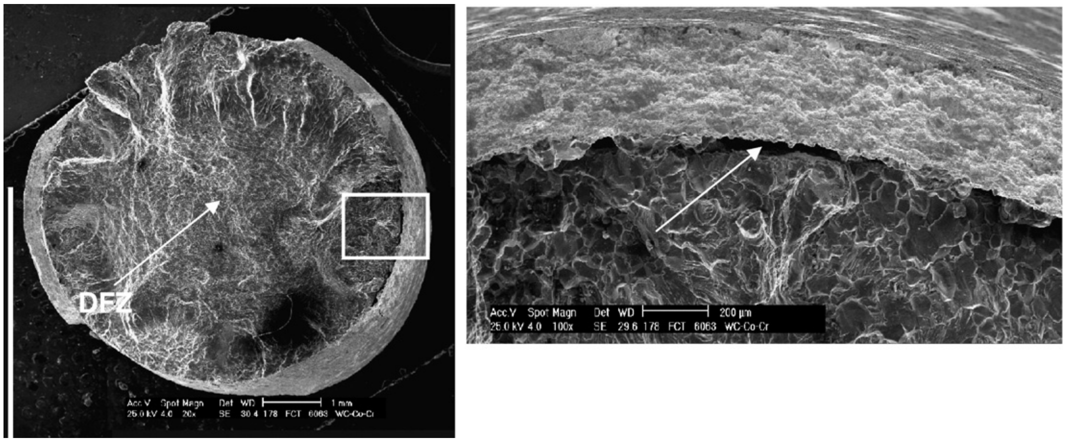

Fig. 7. Fracture surface of a sample tested in NaCl at an alternating stress of 178 MPa, which failed at 128,100 cycles. (a) General view of the surface indicating the position of the ductile fracture zone (DFZ). (b) Detailed view of the area depicted in (a). The arrow indicates the delamination of the coating from the substrate.

mechanical properties and hardness of the aluminum alloy substrate. It has been observed that the WC–10Co–4Cr coating displays a significant indentation size effect and has a mean hardness of ~9.4 GPa.

Acknowledgments

The present investigation has been conducted with the financial support of the Venezuelan National Fund for Science, Technology and Innovation (FONACIT) through the projects S1-2000640, LAB-97000644 and PI-2007000923, as well as the Scientific and Humanistic Development Council of the Universidad Central de Venezuela through the project No. PI 08-00-5793-2005. The authors are also grateful to Plasmatec Ingenieros C. A. (Guarenas, Edo. Miranda, Venezuela), for conducting the coating of the samples employed in the present work.

References

[1] B. Meyers, S. Lynn, ASM Handbook, Surface Engineering, vol. 5, ASM International, Materials park, OH, 1994, p. 925.
[2] K.O. Legg, M. Graham, P. Chang, F. Rastagar, A. Gonzales, B.D. Sartwell, Surf. Coat. Technol. 81 (1996) 99.
[3] R.L. Twite, G.P. Bierwagen, Prog. Org. Coat. 33 (1998) 91.
[4] P.M. Natishan, S.H. Lawrence, R.L. Foster, J. Lewis, B.D. Sartwell, Surf. Coat. Technol. 130 (2000) 218.
[5] H.J. Gibb, P.S.J. Lees, P.F. Pinsky, C.B. Rooney, Am. J. Ind. Med. 38 (2000) 15.
[6] B.D. Sartwell, K. Legg, P.E. Bretz, Proc. Aerospace Plating and Metal Finishing Forum, American Electroplaters and Surface Finishers Society, Cincinnati, OH, USA, March 2000, p. 131.
[7] B.D. Sartwell, K.O. Legg, J. Schell, J. Sauer, P. Natishan, D. Dull, J. Falkowski, Validation of HVOF WC/Co thermal spray coatings as a replacement for hard chrome plating on aircraft landing gear NRL/MR/6170-04-8762, Naval Research Laboratory, Washington, DC, USA, 2004.
[8] B.D. Sartwell, K.O. Legg, A. Nardi, R. Kestler, W. Assink, J. Schell, Replacement of chromium electroplating on C-2, E-2, P-3 and C-130 propeller hub components using HVOF thermal spray coatings, NRL/MR/6170-04-8763, Naval Research Laboratory, Washington, DC, USA, 2004.
[9] O.C. Brandt, Int. J. Fatigue 18 (6) (1996) 417.
[10] R.T.R. McGrann, D.J. Greving, J.R. Shadley, E.F. Rybicki, T.L. Kruecke, B.E. Bodger, Surf. Coat. Technol. 108–109 (1998) 59.
[11] B.J. Connolly, Q. Meng, A.L. Moran, R.L. McCaw, Corros. Eng., Sci. Technol. 39 (2) (2004) 137.
[12] C.J. Kong, P.D. Brown, S.J. Harris, D.G. McCartney, Mater. Sci. Eng., A Struct. Mater.: Prop. Microstruct. Process. 403 (2005) 205.
[13] E.S. Puchi-Cabrera, C. Villalobos-Gutiérrez, I. Irausquín, J. La Barbera-Sosa, G. Mesmacque, Int. J. Fatigue 28 (2006) 1854.
[14] E.S. Puchi-Cabrera, M.H. Staia, J. Lesage, L. Gil, C. Villalobos-Gutiérrez, J. La Barbera-Sosa, E.A. Ochoa-Pérez, E. Le Bourhis, Int. J. Fatigue (2007), doi:10.1016/j.ijfatigue.2007.09.001.
[15] J.A. Marin de Camargo, H.J. Cornelis, V.M.O. Hilário Cioffi, M.Y. Pitanga Costa, Surf. Coat. Technol. 201 (2007) 9448.
[16] E.S. Puchi-Cabrera, R. Maccio, M.H. Staia, Surf. Eng. 22 (4) (2006) 253.
[17] A. Piñeiro-Jiménez, C. Villalobos-Gutiérrez, M.H. Staia, E.S. Puchi-Cabrera, Mater. Sci. Technol. 23 (3) (2007) 253.
[18] V.A.D. Souza, A. Neville, Mater. Sci. Eng., A Struct. Mater.: Prop. Microstruct. Process. 352 (1–2) (2003) 202.
[19] C. Godoy, M.M. Lima, M.M.R. Castro, J.C. Avelar-Batista, Surf. Coat. Technol. 188–189 (2004) 1.
[20] G. Bolelli, R. Giovanardi, L. Lusvarghi, T. Manfredini, Corros. Sci. 48 (11) (2006) 3375.
[21] J. Berget, T. Rogne, E. Bardal, Surf. Coat. Technol. 201 (18) (2007) 7619.
[22] Standard methods of tension testing wrought and cast aluminum and magnesium alloys products, B 557, Annual Book of ASTM Standards, Vol. 03.01, ASTM, Philadelphia, 1984, p. 82.
[23] ASTM E 206-72, Standard definitions of terms relating to fatigue testing and the statistical analysis of fatigue data. 1979.
[24] V.V. Sobolev, J.M. Guilemany and J. Nutting, High-velocity oxy-fuel spraying: theory, structure–properties relationships and applications, The Institute of Materials, Minerals and Mining, Pub. Maney Publishing, London, U.K., 2004.
[25] D. Tabor, The Hardness of Metals, Oxford University Press, Oxford, U.K., 1951.
[26] J.G. La Barbera-Sosa, Y.Y. Santana, M.H. Staia, D. Chicot, J. Lesage, J. Caro, G. Mesmacque, E.S. Puchi-Cabrera, Surf. Coat. Technol. (in press), doi:10.1016/j.surfcoat.2008.04.041.